Journal of Asian Earth Sciences 131 (2016) 95–108

Contents lists available at ScienceDirect

Journal of Asian Earth Sciences

journal homepage: www.elsevier.com/locate/jseaes

Full length article

Role of microfabrics and magnetic fabrics in the tectonic evolution of the Achankovil shear-zone, South India

C. Vikas [a,*], V. Prasannakumar [b], P. Pratheesh [c]

[a] ONGC, Forward Base, Cauvery Asset, Neravy, Karaikal, Pondycherry, India
[b] Department of Geology, University of Kerala, Thiruvananthapuram, Kerala 695 581, India
[c] Department of Geology, School of Earth Science Systems, Central University of Kerala, Tejaswini Hills, Periye, Kasargod, Kerala 671316, India

ARTICLE INFO

Article history:
Received 22 April 2016
Received in revised form 9 September 2016
Accepted 15 September 2016
Available online 16 September 2016

Keywords:
Achankovil shear-zone
Crystallographic lattice preferred orientation
Anisotropy of magnetic susceptibility
Kinematic evolution

ABSTRACT

Achankovil shear-zone, a major crustal discontinuity in South India, which extends for about 120 km in a NW-SE direction, separates the khondalite belt from the terrain of massive charnockites in the north. Progressive mylonitisation and shear fabrics, corresponding to a progression in strain as displayed by grain size reduction, flattening, elongation and dimensional preferred orientation of constituent minerals, characterize the shear-zone. The present work incorporates the results of petrofabric and magnetic susceptibility analyses with a view to interpret the kinematic and microstructural evolution of the shear-zone. EBSD derived LPO suggests plastic deformation through the activation of intracrystalline slip systems and modifications in the fabric due to the reactivation. Magnetic fabric data show significant correlation with the field and LPO fabrics reflecting the regional strain/kinematics and fabric development. The fabrics and kinematic indicators on meso- and microscopic scales reveal dominant dextral shear sense with a minor component of sinistral shearing in micro domains due to strain partitioning and/or reactivation of the shear-zone.

1. Introduction

Shear-zones of the Southern Granulite Terrain (SGT) have gained significance in global tectonics, in terms of their prominent role in supercontinental assemblies, especially the Proterozoic East Gondwana reconstruction. However, the movement picture of shear-zones in the broken and relocated constituent continents often impose constraints in arriving at the reassembly with best fit of the supercontinents. The South Indian Shield, a mosaic of several accreted tectonic blocks with contrasting geological and geochronologic signatures, is dissected by two major Proterozoic shear systems (Drury and Holt, 1980; Drury et al., 1984; Chetty et al., 2003), the Palghat-Cauvery and the Achankovil (Fig. 1). The Achankovil shear-zone (AKSZ), a NW–SE trending strike slip shear-zone of late Proterozoic age, situated in the southern part of the SGT, is conspicuous in the satellite imageries and aero magnetic data (Drury and Holt, 1980; Drury et al., 1984; Reddi et al., 1988). It is 8–10 km wide and can be traced for about 120 km starting from the west coast (Prasannakumar, 1998). This transcrustal lineament figures as the boundary between the vast supracrustal belt of granulite-grade metapelites of the Trivandrum Block (TB) in the south and the charnockite enderbite-gneiss suite of the Madurai Block (MB) in the north and defines the prominent magnetic, lithological, and isotopic limits (Santosh, 1987; Brandon and Meen, 1995; Rajaram et al., 2003).

The renewed global interest in granulite petrogenesis as well as Gondwana correlation has focused attention on lithologies of both sides of the AKSZ which has been generally correlated to the Ranotsara shear-zone (e.g., Windley et al., 1994; Rajesh et al., 1998) and dextral Angavo shear-zone (Raharimahefaa and Kusky, 2010) in Madagascar. Achankovil shear-zone has been variously treated as a neo-tectonic expression (Sinha Roy et al., 1984; Radhakrishna et al., 1990), geosuture (Srikantappa et al., 1985; Rajaram and Anand, 2014), shear-zone (Santosh, 1987), lineament (Reddi et al., 1988) or intracratonic litho-tectonic feature (Kumar et al., 2009). Shearing in the AKSZ has been described as dextral (Sacks et al., 1997) as well as sinistral (Rajesh et al., 1998; Rajesh and Chetty, 2006) based on mesoscopic shear sense indicators and thus the kinematic evolution of this crustal-scale structure is debated. The opposing views existing on the dextral/sinistral slip along the AKSZ jeopardize the attempts of demonstrable correlation of super continents. Thus the characterization of the shear-zone and its kinematic interpretation remain a challenge. The

* Corresponding author.
E-mail address: vikascnair@gmail.com (C. Vikas).

http://dx.doi.org/10.1016/j.jseaes.2016.09.011
1367-9120/

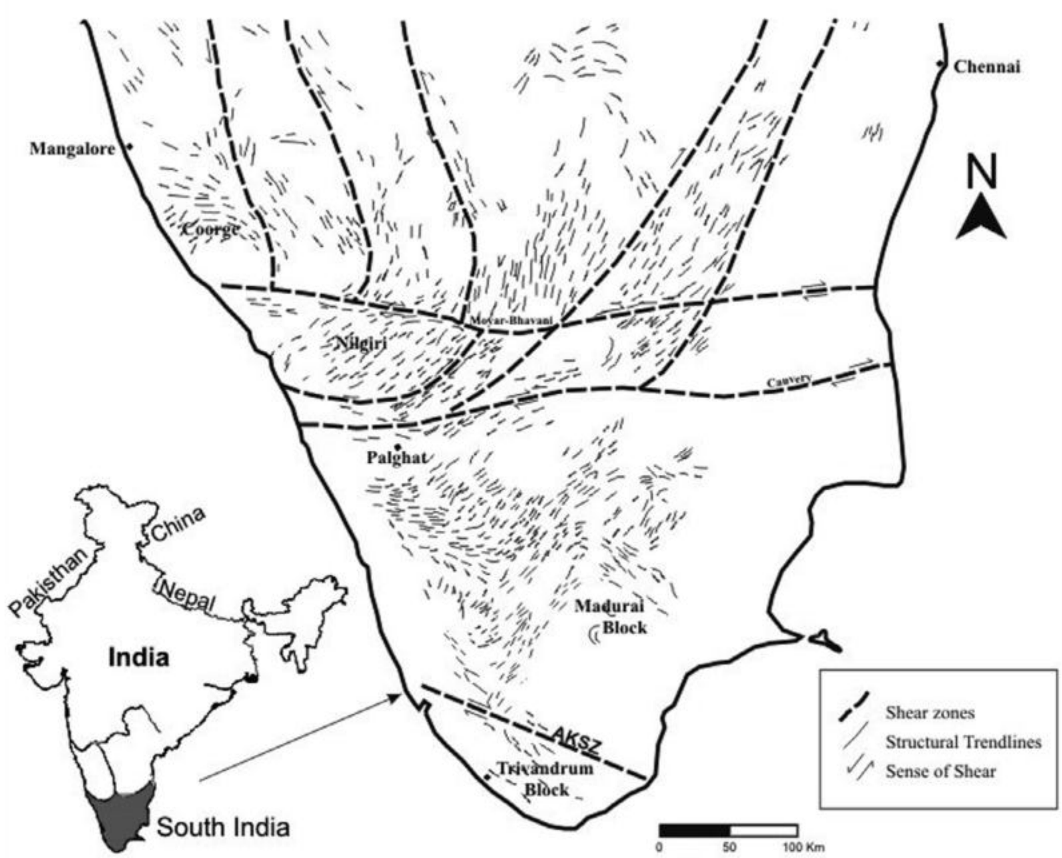

Fig. 1. Tectonic map of South India with disposition of shear zones (modified after Drury and Holt, 1980).

systematic field investigations across the area, especially along a major part of length and width of the zone, falling in the states of Kerala and Tamilnadu, indicate that there exists a distinct zone of highly sheared gneisses with numerous kinematic indicators and hence it can be considered as a shear-zone. However, the dearth of widely exposed LS fabrics, a common constrain in high grade metamorphic terrains, impedes an acceptable kinematic analysis. In such cases, microfabrics and magnetic fabrics, when used in conjunction with the mesoscopic fabrics, have proved to be significant proxies for tectonite fabrics. Hence, the present work is an attempt to bring out the geology and structural geometry of the shear-zone with a view to interpret its kinematic and microstructural evolution, incorporating the results of microfabric and magnetic susceptibility analyses.

2. Geological setting

The important rock types within the AKSZ are deformed and highly migmatised garnet-biotite gneiss, cordierite gneiss, mylonite, charnockite (both massive and patchy), calc-granulite, marble, pyroxene granulite and younger intrusives such as granite, gabbro and dunite (Fig. 2). These rocks, except the intrusives, have been mylonitised and retrogressed, especially along shear planes and usually have a gradational contact between them. The mylonitic fabric is well exhibited by the quartzofeldspathic and calcareous rocks and in the proximity of shear-zones the regional gneissic fabrics become progressively destroyed. Within the belts of high shearing strain, all stages of transition from protomylonite to ultramylonite can be seen. This gradation varies from place to place due to heterogeneous composition of the rocks.

3. Mesoscopic structures

A strong, tectonic L-S fabric has developed all along the AKSZ. The AKSZ is distinctly defined by NW–SE trending planar fabrics (Fig. 3) with moderate to steep dips to SW. The general structural grain is controlled by mutually parallel compositional layering (S_0) and foliation (S_1) striking NW-SE and dipping moderately-to-steeply (40^0–85^0) towards NE or SW (Fig. 3). The most widely developed planar fabric is a penetrative foliation (S_1) after crystals of hornblende, flakes of biotite and flattened grains of quartz and feldspar. The earlier planar fabrics, S_0 and $S_{1,}$ were deformed by younger asymmetrical F_2 folds (Fig. 4a), plunging NW or SE. Coaxial nature of F_1 and F_2 suggests their development during a progressive deformation event. The shear-zone fabric is controlled by the penetrative mylonitic foliation S_2 (Fig. 4b), defined by flakes of biotite and flattened and elongated polycrystalline aggregates of quartz and feldspar. In sheared and strongly foliated rocks, S_2 planes are overprinted by regularly or irregularly spaced shear band cleavages (C′ planes, Fig. 4c), dominantly striking NE–SW. The presence and occurrence of tight to isoclinal intrafolial folds within the mylonites and the parallelism of mylonitic foliation (S_2) and fold axial surfaces strongly advocates that the mylonitic foliation represents the principal flattening plane. The strong flattening of fabrics parallel to the shear plane indicates simple shear deformation. The mylonitic lineations of AKSZ have low plunges towards NW/SE. The low plunge of the lineations on the steep mylonitic foliation surface indicates a large strike-slip component for the shear-zone. Within the shear-zone, the mylonitic foliation is itself deformed to broad open folds with axial surfaces sub parallel to the F_3 folds (Fig. 4d) developed in gneisses that occur outside the shear-zone. The structures of the study area thus indicate

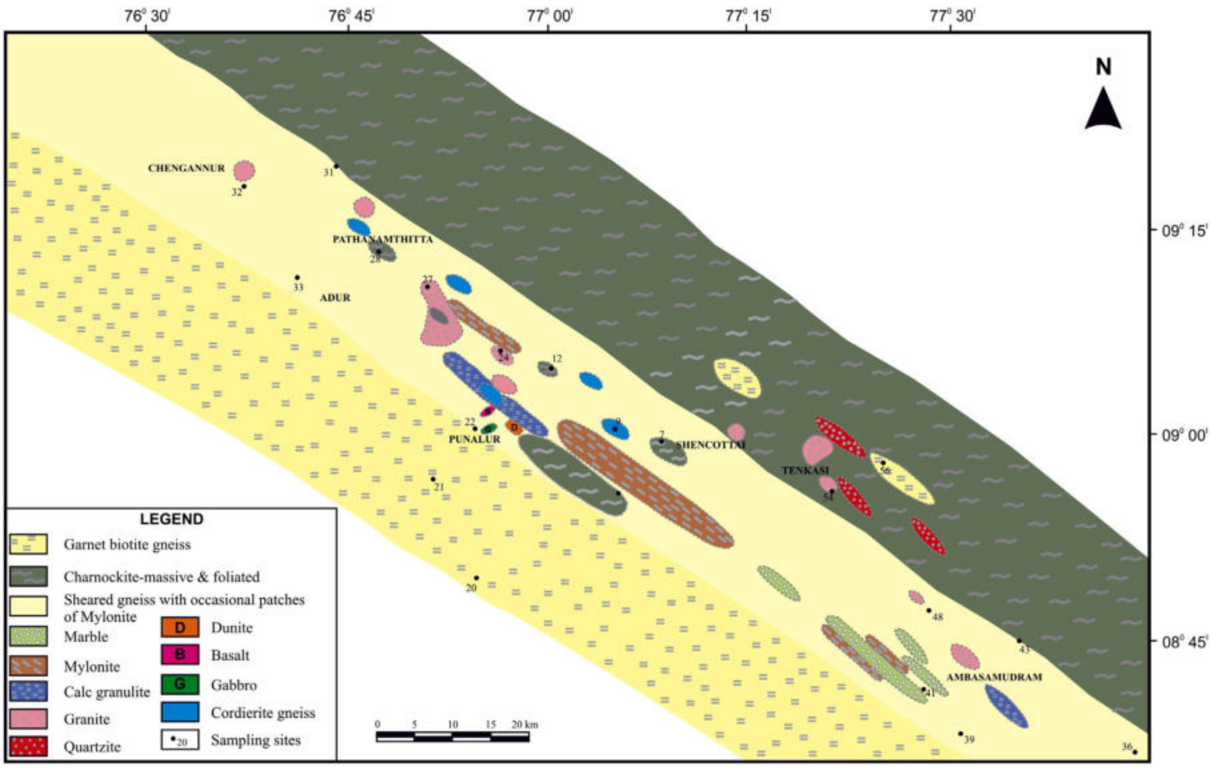

Fig. 2. Geological map of the study area with AMS sampling sites.

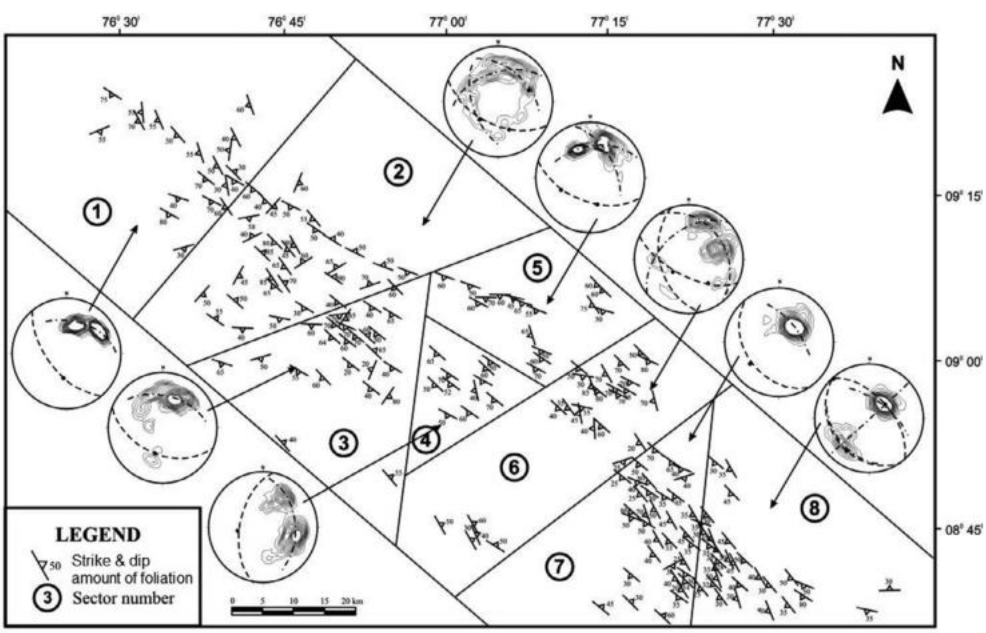

Fig. 3. Foliation (S_1) map of the study area. S_1 pole diagrams for the respective eight sectors are also shown.

their formation in the course of three major deformational events – D_1, D_2 and D_3. The shearing which began in the D_2 was reactivated during D_3. Metamorphic recrystallisation was mostly completed before the onset of D_3 event. Extensional structures such as composite planar fabric, pinch and swell structures (Fig. 4e), foliation boudinage (Fig. 4f) and rotated boudins are well developed during the ductile shearing event.

4. Microscopic structures

Polyphase deformation and metamorphism accompanied by shearing have given rise to different textural variants of mylonites in AKSZ. Mylonitic to ultramylonitic fabric characterizes the bulk of the shear-zone and there is a progressive increase in foliation intensity towards the mylonitic zones. The variants correspond

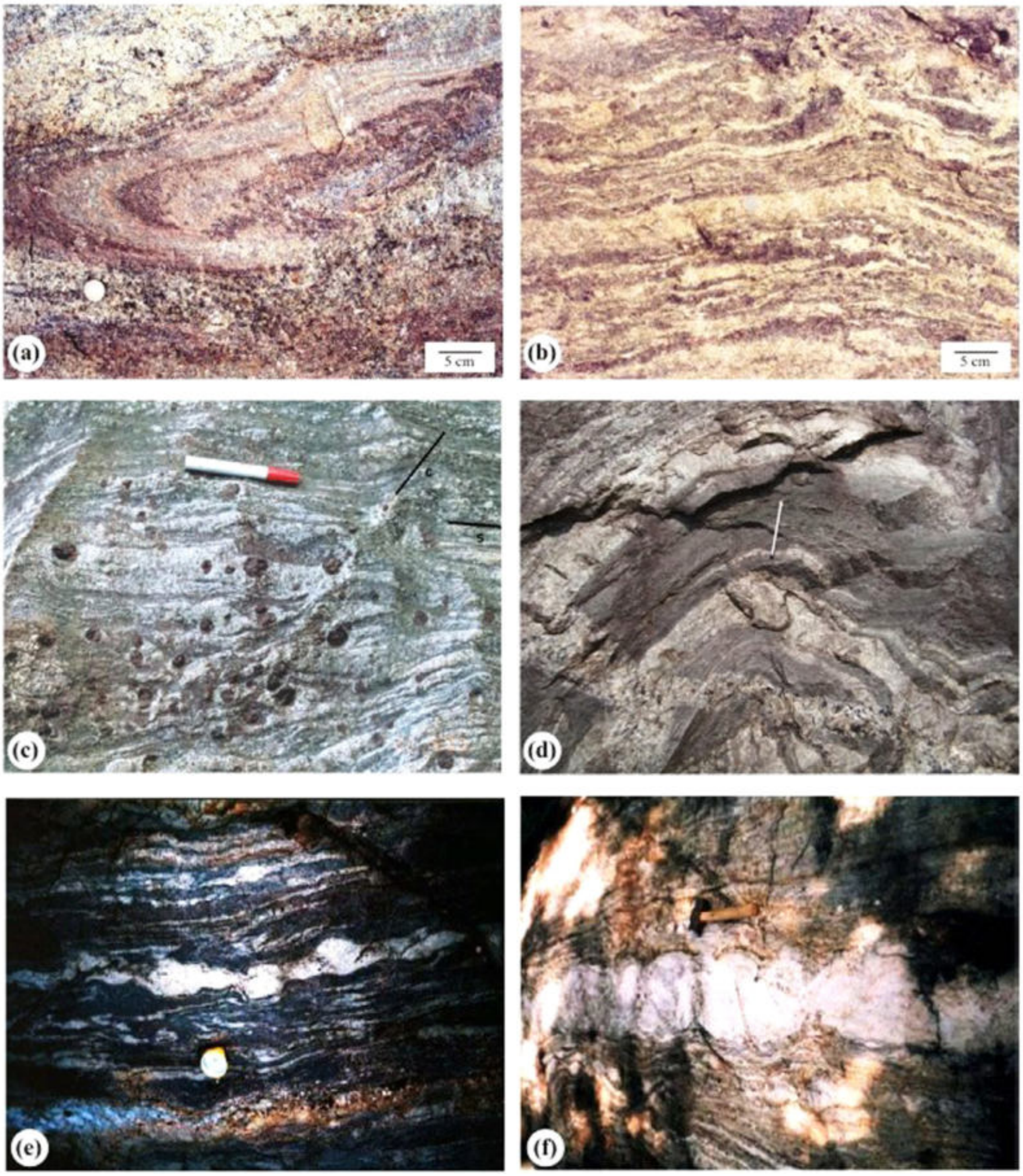

Fig. 4. Mesoscopic structures in the study area: (a). Minor F_2 fold on both foliation (S_1) and compositional layering (S_0). Note the modification of fold limbs by F_3 folding (Plan view) (b). Closely spaced mylonitic foliation (Vertical section) (c). S-C fabric in garnet biotite gneiss defining sinistral shear sense (Inclined section) (d). Broad open F_3 folds in the study area (Inclined section) (e). Pinch and swell structures in gneiss. Note the necking and pinching of quartz rich layers (Inclined section) (f). Foliation boudinage in garnet biotite gneiss (Plan view).

to a progression in strain manifested by grain size reduction and increasing flattening and elongation of polycrystalline quartz, feldspar and hornblende-biotite rich layers. Three principal types of microstructures were recognised: preserved fabrics outside the shear-zone (Type-1), partly recrystallised shear-zone-fabrics (Type-2) and reequilibrated shear-zone-fabrics (Type-3).

The Type-1 fabric, marked by the rocks outside the shear-zone, is broadly gneissic in nature and contains large unoriented feldspar grains together with biotite and quartz. Weakly deformed quartz grains showing weak undulose extinction and a deviation from equidimensionality revealing low strain values have been noticed. Microstructurally, protomylonites (Fig. 5a) are much similar to the protolith. The protomylonite is coarse grained and has undergone little grain refinement. Individual grains have straight or slightly curved grain boundaries and the shape preferred orientation is ill-defined. These features suggest that these rocks have not been affected by shearing.

Near the shear-zone boundary, Type-2 fabric is represented by porphyroclastic mylonite (Fig. 5b) and mylonite showing signs of dynamic recrystallisation and decrease in grain size as compared to the coarse-grained Type-1 fabric. The mylonite (Fig. 5c) is finer grained than the protomylonite and the porphyroclastic mylonite. The dominant two grain-size population is completely replaced by an approximately homogeneous grain population and the grain refinement is even more evident during this stage. S_1 is progressively rotated into parallelism with S_2 and a shear band C′ develops at an angle. Among quartz and feldspar porphyroclasts, quartz grains are more elongated and the development of sub grains within the quartz results in crude banding (Fig. 5d). In quartz rich domains, elongated ribbon like quartz is predominant (Fig. 5c). Quartz grains also show fair development of deformation bands and undulose extinction (Fig. 5d). Feldspars like plagioclase and orthoclase occur either as large porphyroclasts or as small grains in the groundmass. Large porphyroclasts of plagioclase show well

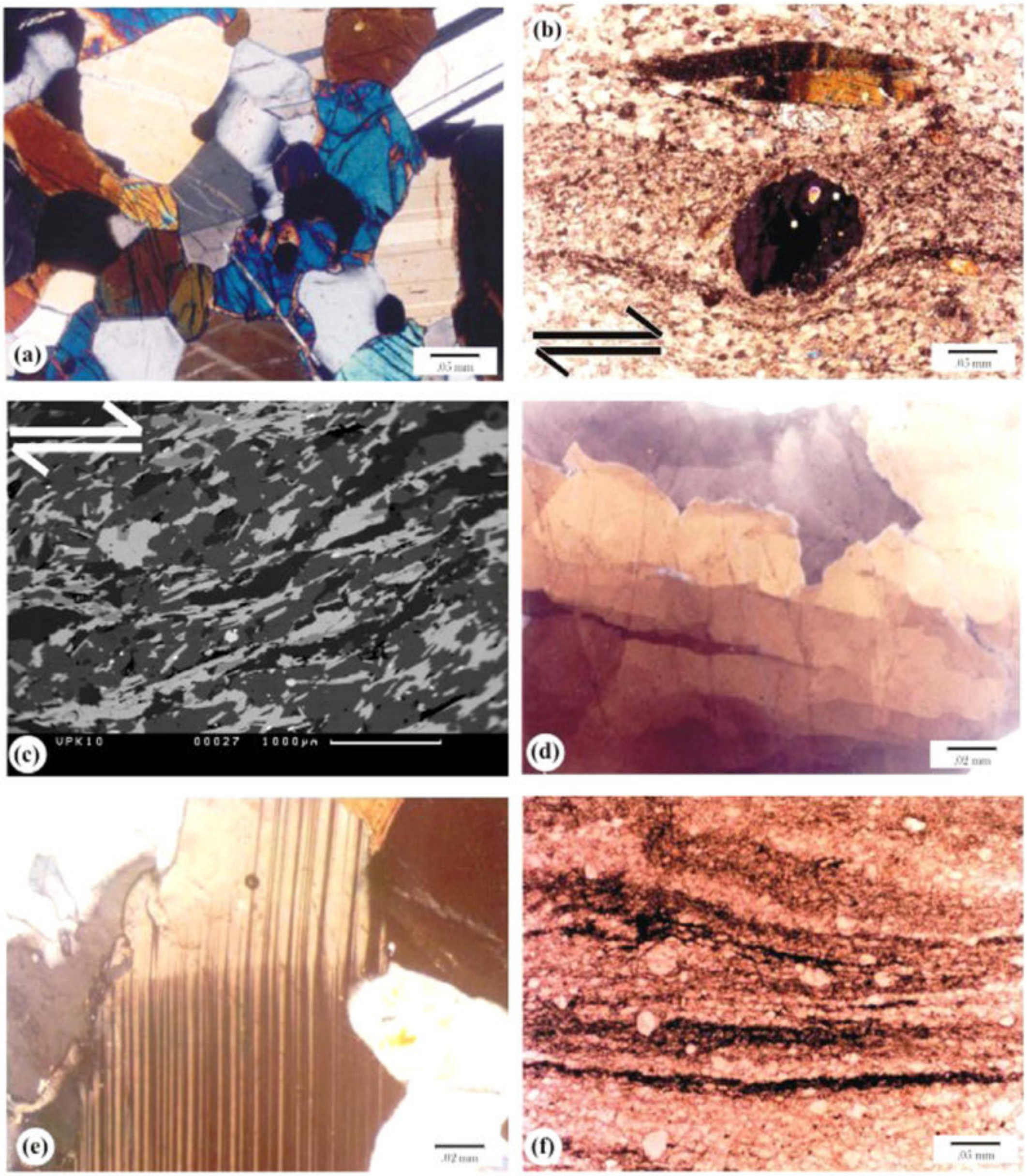

Fig. 5. Microscopic structures in the study area: (a) Protomylonite. Note the straight or slightly curved grain boundaries (Crossed nicols). (b) Mylonitic foliation swerving around garnet porphyroblast indicates dextral shearing. Dragged out mica porphyroclasts are also noticed (Crossed nicols). (c) SEM image showing mylonitic fabric with elongated, sigmoidal quartz ribbons and small biotite flakes defining foliation. (d) Prism subgrain boundaries in quartz. Note the undulose extinction experienced by the quartz grains (Crossed nicols). (e) Bent and curved twins in plagioclase. Also note the wavy extinction shown by plagioclase lamellae (Crossed nicols). (f) Fine grained ultramylonite. Note the sub-parallel C-band structure (Crossed nicols).

developed features characteristic of ductile deformation like wavy extinction (Fig. 5e), deformation twinning, bending (Fig. 5e) as well as kinking of twin lamellae and sub grain development. At many places, they are seen to be fractured and displaced with recrystallised grains near the margin. Recrystallisation nearer to the grain boundaries of the deformed grains lead to the formation of core and mantle structure (White, 1976) with a fine-grained recrystallised mantle surrounding a strained megacryst.

Type-3 fabric is characterised by ultramylonites showing uniform grain-size, a well-equilibrated feldspar microstructure and mineral assemblage (biotite replacing garnet) indicating amphibolite facies retrograde conditions. Progressive shearing results in rotation of C′ into parallelism with foliation planes and finally they merge to form a complex mylonite fabric in the ultramylonite stage (Fig. 5f). K-feldspar exhibits twinning. Quartz ribbons are strongly elongated and show signs of intense plastic deformation. Quartz has suffered greater recrystallisation and sub grain development as a result of intense shearing.

5. Lattice preferred orientation

5.1. Sampling and analytical methods

Crystallographic preferred orientation (CPO) analysis of major minerals is a useful tool for understanding the widespread deformation processes in orogens and it provides 3-D information about kinematics of deformation. The present work describes the CPO in the sheared rocks from the AKSZ, measured via Universal stage techniques (Turner and Weiss, 1963) and SEM electron backscatter diffraction (EBSD) (Prior et al., 1999). Oriented thin sections were prepared from 26 oriented samples of garnet biotite gneiss and mylonitic gneiss from different parts of the study area. Quartz c-axis and poles to (001) of biotite were measured by standard Universal stage techniques (Turner and Weiss, 1963) using oriented thin sections cut parallel to the XZ plane of the strain ellipsoid. In this reference frame, foliation is assumed to represent the XY plane of the finite strain ellipsoid and lineation which lies in the plane of foliation, represents the direction of the maximum finite elongation (X). The data have been plotted on an equal area lower hemisphere projection (Schmidt net) and are contoured following the Kamb method with $E = 3\sigma$. In the fabric diagrams, X and Z are oriented E-W and N-S respectively; Y being at the centre.

One representative garnet biotite gneiss sample (VPK10) from the shear-zone rocks was chosen for EBSD analysis of plagioclase, orthoclase, hornblende, biotite and quartz. The samples were prepared following conventional procedures (Lloyd, 1987) and analysed via automated EBSD using the *HKL Channel 5* software package (Schmidt and Olesen, 1989) on a *CamScan Series-4* SEM at the University of Leeds, UK, using standard SEM operating conditions as described in Prasannakumar and Lloyd (2007). The Crystal Lattice Preferred Orientation (LPO) pole figures are represented in lower hemisphere, equal-area projections in which the plane of projection is XZ ($X \geqslant Y \geqslant Z$), with X and Z oriented 'E-W' and 'N-S' respectively (Fig. 6). The mylonitic stretching lineation is parallel to X, while the foliation is vertical and trends E-W such that Y is perpendicular to the plane of projection and hence lies at the centre of each pole figure. The strength of each LPO distribution is indicated by the pfJ-value (Bunge, 1982). A random distribution of LPO is indicated by the pfJ-value of 1.0 (Michibayashi and Mainprice, 2004). In general, biotite and hornblende exhibit the strongest LPO whereas the orthoclase LPO is significantly stronger than plagioclase and quartz is very weak.

5.2. Results

Quartz c-axis pattern in the garnet biotite gneiss samples of the study area, measured by standard Universal stage techniques, is characterised by a pronounced maximum lying at small angles to the pole to mylonitic foliation, with the minimum either close to mylonitic foliation or at low angles from it (Fig. 7a–h). The *quartz* CPO based on EBSD data of garnet biotite gneiss sample is characteristically weak, as evidenced by the pfJ-values that are only slightly greater than unity ranging from 1.04 to 1.30 (Fig. 6a). The [0001] and rhomb CPO are slightly more organized with the (0001) defining weak girdle distribution sub-parallel to foliation, with maxima subparallel to X tectonic direction. However, the typical pattern of preferred orientation in mylonites of the study area is characterised by the peripheral maximum of [0001] axes inclined at 42^0–64^0 to X and are asymmetrically aligned with trace of foliation (Fig. 7i–l). The rhomb CPO exhibits more or less opposite distributions for $(10\bar{1}1)$ and $(01\bar{1}1)$ with the former developing a maximum parallel to Z and a girdle distribution of equivalent density parallel to XY, the foliation (Fig. 6a).

Plagioclase non-polar data on lower hemisphere projections exhibit typically weak LPO (Fig. 6b), characterised by pfj-values close to unity. The development of a weak girdle distribution of (100) parallel to XY is indicated by Fig. 6b.

The EBSD data suggest that *biotite* has the strongest LPO (Fig. 6c), characterised by a well defined peripheral maxima of [001] parallel to Z such that the (001) cleavage plane of biotite defines the foliation plane. The poles to (001) of biotite in gneiss, measured by standard Universal stage techniques, also form incomplete peripheral girdle about Y with a compact maximum, normal to S_1 foliation (Fig. 8). EBSD data indicate that both (010) and (100) are constrained to lie within this foliation plane, forming girdle distributions (with concentrations) parallel to foliation (XY). The maximum in (010) is parallel to Y with sub maxima close to X. Similar behaviour is shown by (100) which exhibits a weak cluster subparallel to Y and weak girdle distributions subparallel to XZ (Fig. 6c).

Hornblende LPO is characterised by a maximum in [001] parallel to Y and defines incomplete girdle distribution parallel to foliation (XY). The (100) is more dispersed with a weak maximum subparallel to Y and exhibits weak girdle distributions subparallel to both YZ and XY respectively (Fig. 6d). Much weaker girdles parallel to XZ are shown also by (010), having a maximum subparallel to Z tectonic direction.

In the *Orthoclase* LPO, (100) is characterised by weak and complex distribution lacking organisation. It exhibits a weak maximum subparallel to Z, suggesting the orientation of (100) planes subparallel to the foliation (Fig. 6e). The (010) and (001) are also dispersed and the former defines a nearly complete great circle girdle distribution subparallel to foliation, with a maximum subparallel to Y. The (001) also defines an incomplete peripheral girdle distribution subparallel to both XY and YZ with a maximum inclined to X.

6. Anisotropy of magnetic susceptibility (AMS)

6.1. Sampling and analysis

The anisotropy of magnetic susceptibility (AMS) is applied for different aspects of petrofabric analysis of rocks because the magnetic fabric reflects the preferred orientation of the crystal lattice and shape of magnetic minerals in a rock. Three oriented core samples of 7 cm length and 2.5 cm in diameter were drilled out from each of the 19 locations, across the area, using a portable hand corer. These samples were later cut into 2.2 cm long pieces and analysis of low-field AMS ($200\ Am^{-1}$) using an advanced MFK1-A Kappabridge of *AGICO*, Brno, was performed at the Structural Geology Laboratory of the Department of Geology, University of Kerala. The analysis provides orientation and magnitude of three principal axes of the magnetic susceptibility ellipsoid ($K_1 > K_2 > K_3$), the mean magnetic susceptibility (K_m), degree of magnetic anisotropy (P') and shape parameter (T). The mean magnetic susceptibility ($K_m = 1/3\ (K_1 + K_2 + K_3)$) is an indicator of the minerals that control the magnetic fabric of a rock. P' measures the eccentricity of the magnetic susceptibility ellipsoid which can be used as an indicator of intensity of deformation while T represents the shape of the susceptibility ellipsoid as oblate or prolate (Jelinek, 1981). The magnetic lineation and foliation are represented as the K_{max} and the plane normal to the K_{min} (K_1–K_2 plane), respectively (Tarling and Hrouda, 1993). The core samples of the study area were subjected to petrographical studies to understand the source of anisotropy carrier for the development of AMS fabric. The results are summarised in Table 1.

6.2. Magnetomineralogy and anisotropy

The massive charnockites generally have very high mean susceptibilities, mostly higher than $10{,}000 \times 10^{-6}$ SI. The mean susceptibility values of massive charnockite vary between 11,248 to $30{,}166 \times 10^{-6}$ SI (Table 1). Similarly, foliated charnockites from the study area also show very high K_m values ranging from 3777 to $38{,}020 \times 10^{-6}$ SI. Garnet biotite gneiss shows lower mean susceptibility values ranging from 38 to 489×10^{-6} SI except in one sample ($K_m > 500 \times 10^{-6}$ SI). Garnet biotite gneiss from location No.48 (Table.1) shows very high K_m values around $20{,}000 \times 10^{-6}$ SI (Fig. 9a). The wide range in the mean susceptibility values indicates variations in the magnetic mineralogy which are also evident

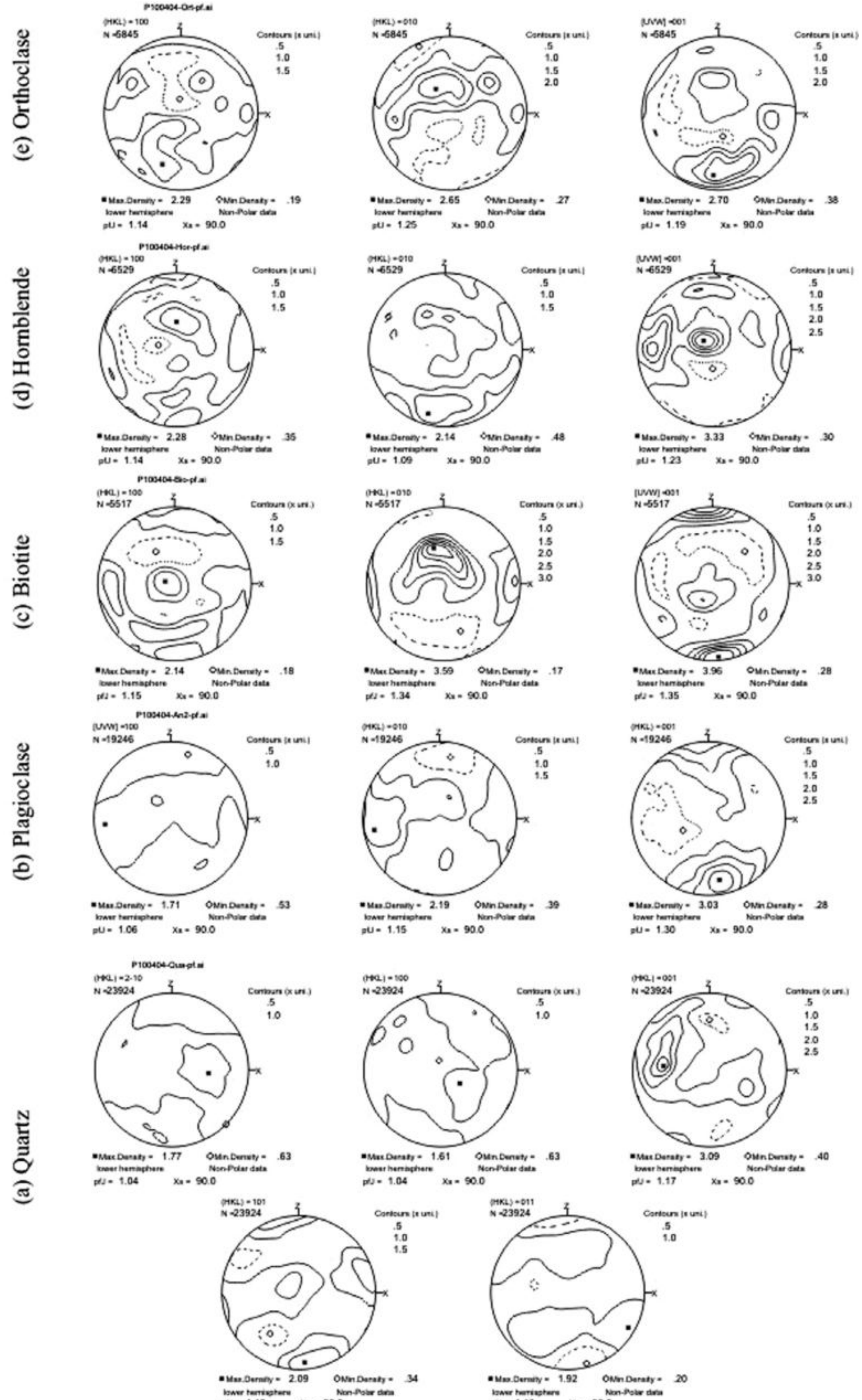

Fig. 6. Individual mineral non-polar data, equal area and lower hemisphere projection LPO pole figures for sample VPK10. All contours are multiples of mean uniform distribution (m.u.d.); 0.5 m.u.d. contour represented by broken lines; solid square, maximum value; open circle, minimum value. Also shown are values of pfJ for each pole figure. In each pole figure, X is oriented E-W, with Z oriented N-S. (a) Quartz $(2\bar{1}\bar{1}0)$, $(10\bar{1}0)$, (0001), $(10\bar{1}1)$ and $(01\bar{1}1)$. (b) Plagioclase [100], (010) and (001). (c) Biotite (100), (010) and [001]. (d) Hornblende (100), (010) and [001] and (e) Orthoclase [100], (010) and (001).

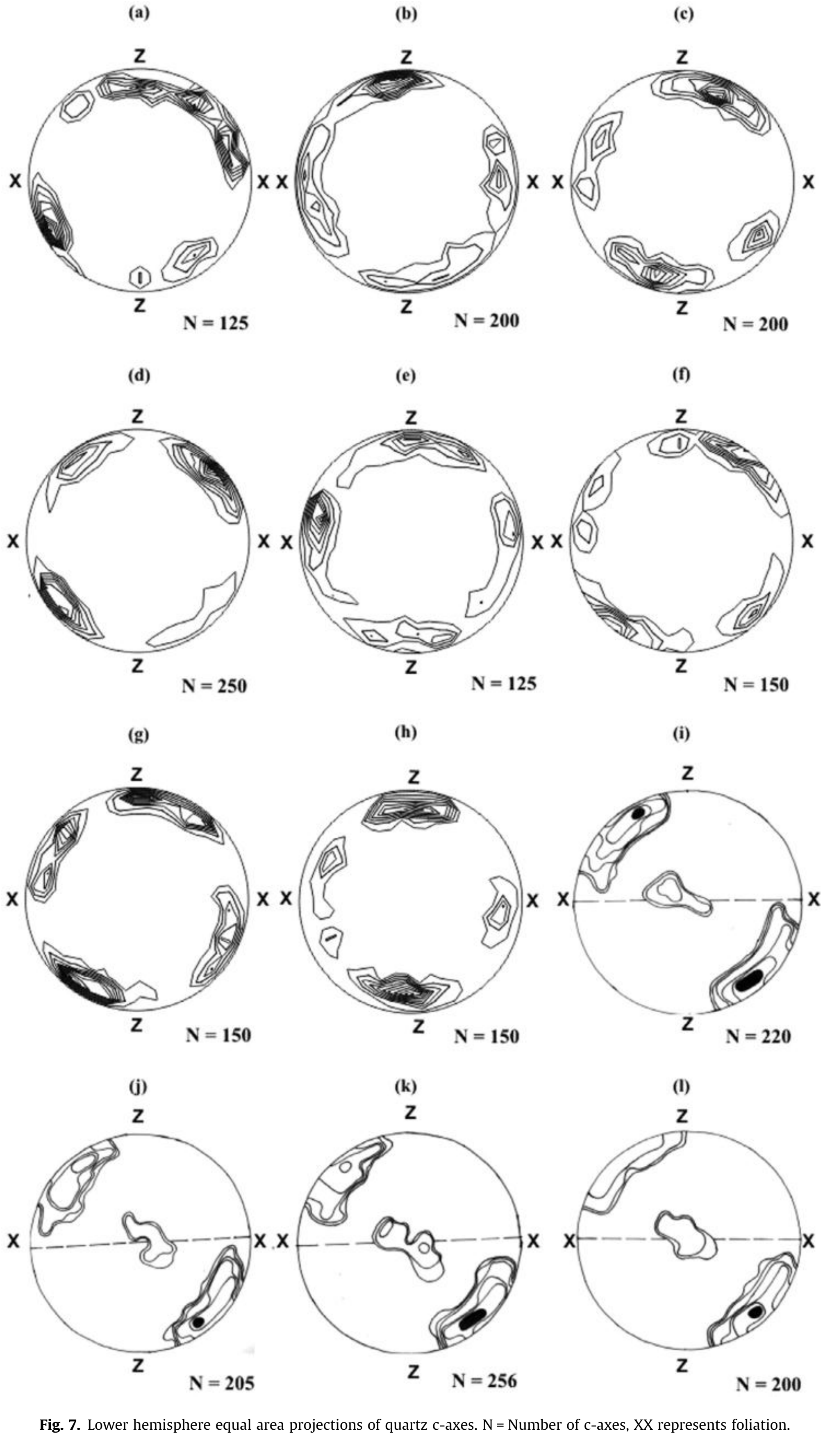

Fig. 7. Lower hemisphere equal area projections of quartz c-axes. N = Number of c-axes, XX represents foliation.

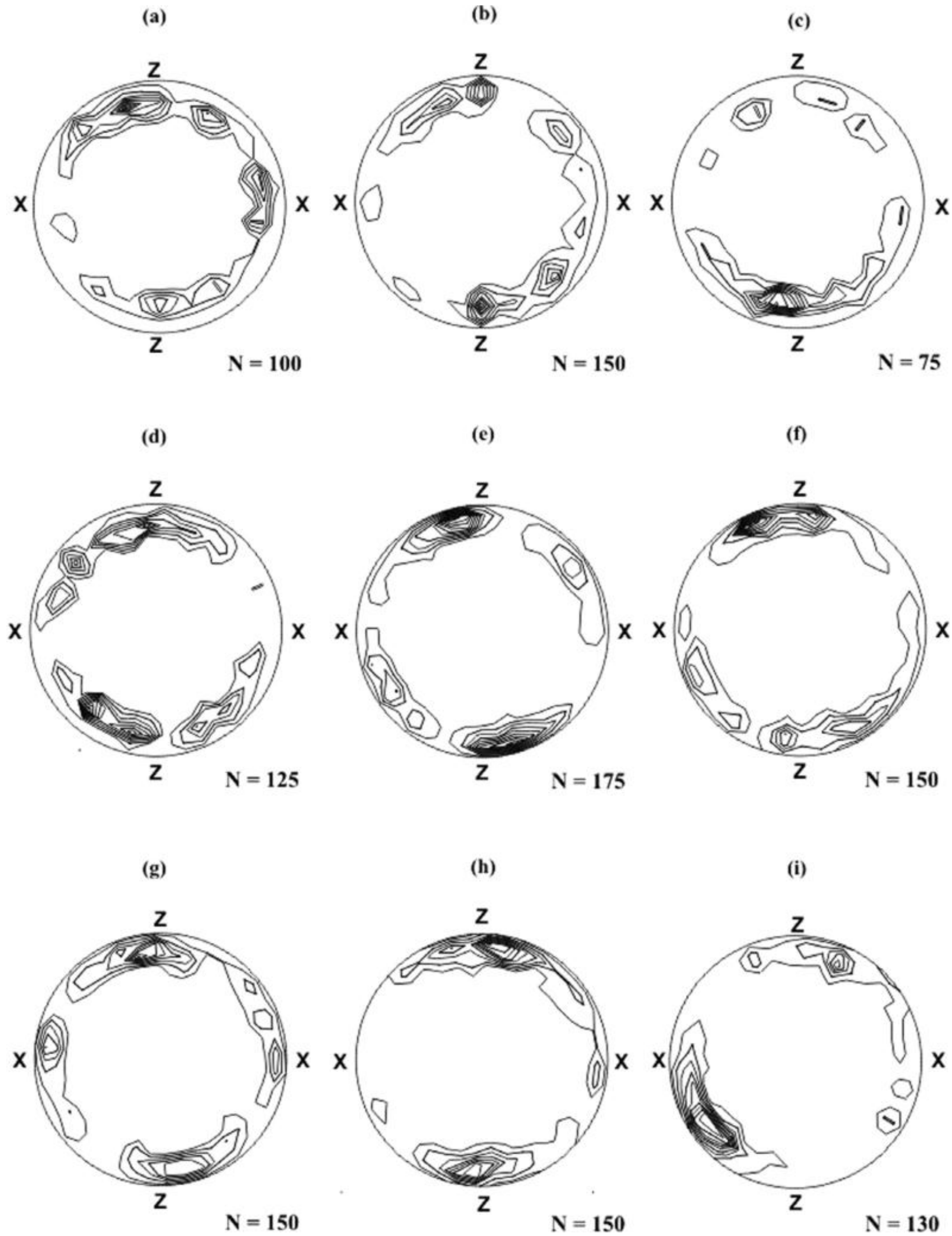

Fig. 8. Lower hemisphere equal area projections of poles to (001) of biotite. N = Number of measurements, XX represents foliation.

in petrographic analysis of the rock samples. The higher values of mean susceptibility of charnockites imply its ferrimagnetic character. The low magnetic susceptibility values (<500 $\times$ 10^{-6} SI) arise from the contribution of the dia- and paramagnetic contributors while the medium to high values result from the presence of varying amounts of ferrimagnetic magnetite with minor fractions of paramagnetic minerals such as hypersthene (Fig. 5a) and biotite. The low to medium susceptibility values noticed in the sheared gneisses may be mainly due to the abundance of paramagnetic minerals like biotite, as evident in petrographic studies (Fig. 5c).

The corrected degree of anisotropy (P') across the 19 locations from the study area ranges from 1.01 to 1.85 (Table 1). In massive charnockites, P' varies from 1.21 to 1.40 (average = 1.31). Similarly, in foliated charnockites, it ranges from 1.23 to 1.85 (average = 1.4). Garnet biotite gneiss shows lower values ranging from 1.02 to 1.5 (average = 1.09) as compared to massive charnockites and foliated charnockites. The anisotropy factor, P', is commonly used as strain intensity gauge which is indicative of the degree of deformation (Rathore, 1980; Tarling and Hrouda, 1993; Archanjo et al., 1995). Hrouda (1993) also investigated mathematically the relationship between strain and P' values for ductile, passive, plane and viscous models. The P' was found to increase with the increase in strain for all the cases and the relationship has been found to hold true even for ferromagnetic minerals such as hematite and magnetite (Hrouda, 1993). In the study area, P' varies between 1.01 (location-39) and 1.85 (location-28). The overall high mean P'

Table 1
AMS data for rocks of the study area.

Loc No.	Sample No.	No. of cores	Rock type	Azi/Dip	K_m (10^{-6} SI)	*L*	*F*	*E*	*P′*	*T*	K_1 (D/I)	K_2 (D/I)	K_3 (D/I)	MF[a]
5	V1	5	Charnockite	225/50	30166.00	1.15	1.04	0.90	1.21	−0.57	106/12	198/12	260/72	350/18
8	V3	5	Charnockite	0/50	17780.00	1.18	1.22	1.04	1.44	0.11	180/24	120/12	12/60	102/30
11	V5	5	Charnockite	195/50	11247.50	1.11	1.10	0.99	1.22	−0.07	315/18	50/18	200/66	290/24
31a	V13	4	Charnockite	30/10	26813.33	1.23	1.12	0.92	1.38	−0.28	340/54	108/30	213/24	303/66
7	V2	4	Foliated charnockite	120/55	3777.20	1.15	1.05	0.91	1.23	−0.39	104/48	290/18	249/48	339/42
12	V6	4	Foliated charnockite	0/0	33690.00	1.08	1.06	0.98	1.16	−0.09	345/66	215/18	114/24	204/66
28	V12	5	Foliated charnockite	100/70	38020.00	1.13	1.59	1.41	1.85	0.59	167/6	120/42	235/42	325/48
9	V4	4	Foliated charnockite	160/68	25255.00	1.06	1.16	1.09	1.24	0.43	350/18	257/6	188/72	278/18
20	V7	4	Garnet biotite gneiss	350/60	391.50	1.01	1.05	1.04	1.06	0.65	97/12	195/42	353/42	83/48
21	V8	5	Garnet biotite gneiss	230/25	153.92	1.07	1.04	0.97	1.13	0.08	137/6	240/54	43/48	313/42
22	V9	4	Garnet biotite gneiss	280/60	489.13	1.01	1.01	1.00	1.02	−0.20	175/24	69/12	10/72	100/18
32	V14	4	Garnet biotite gneiss	110/40	330.85	1.01	1.01	1.01	1.02	0.47	345/18	154/48	293/36	23/54
33	V15	3	Garnet biotite gneiss	70/20	37.55	1.02	1.02	1.00	1.04	0.07	133/6	42/12	240/78	330/12
36	V16	4	Garnet biotite gneiss	40/20	122.08	1.02	1.02	1.00	1.04	0.18	148/0	40/72	240/18	330/72
41	V18	4	Garnet biotite gneiss	70/50	115.54	1.01	1.01	1.00	1.02	−0.02	160/72	282/12	22/18	112/72
43	V19	5	Garnet biotite gneiss	250/40	303.48	1.01	1.04	1.02	1.05	0.46	154/6	264/60	60/24	150/66
48c	V20	4	Garnet biotite gneiss	170/50	20443.33	1.30	1.12	0.86	1.48	−0.37	0/90	210/18	70/6	160/84
39	V17	4	Garnet biotite gneiss	50/40	57.14	1.00	1.00	1.00	1.01	−0.05	0/54	336/30	245/54	335/36
56	V22	4	Garnet biotite gneiss	350/25	111.54	1.05	1.04	0.99	1.10	−0.18	285/66	78/12	172/0	262/90

[a] Magnetic foliation (strike/dip amount).

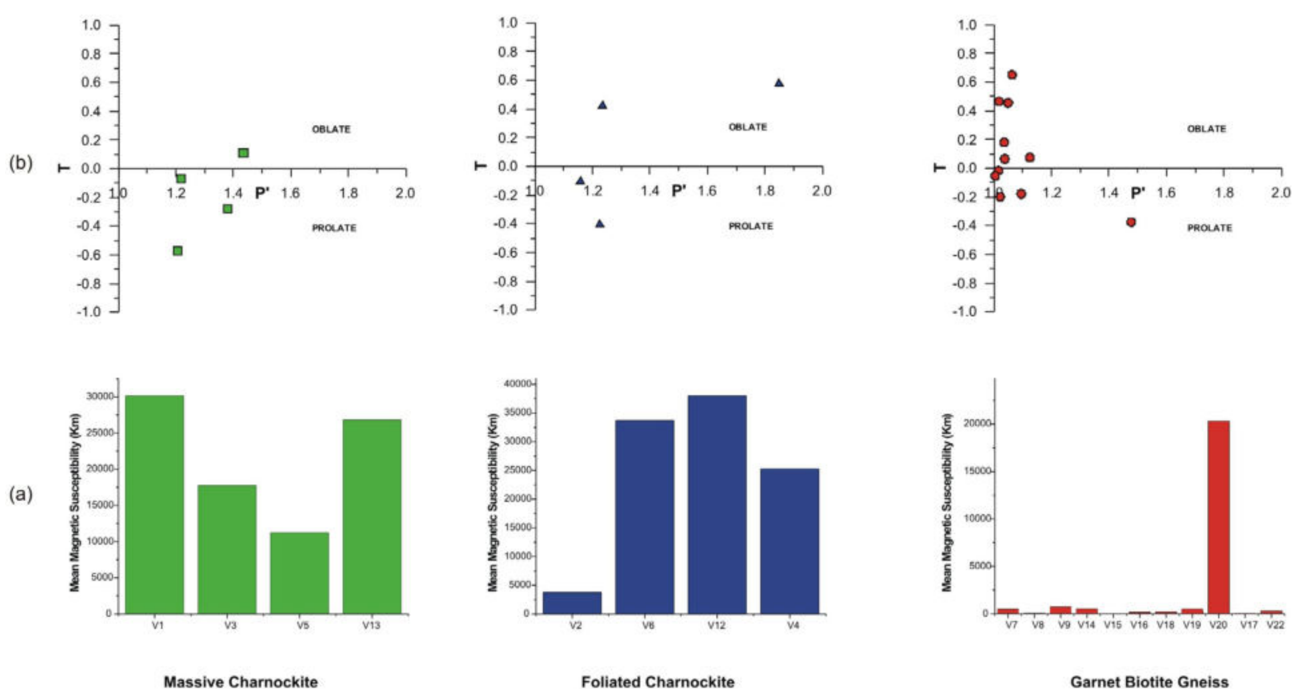

Fig. 9. (a) Bar charts representing magnetic susceptibility (K_m) measured in different rock types and (b) Jelinek plots for different lithologies of the study area.

value of 1.3 is calculated from locations-32, 28, 12, 9, 7 and 48 (Fig. 2) falling at the central part of the shear-zone. Their *P*′ values are relatively high, compared to the other adjacent locations, indicating local intense deformation. This is in agreement with the microstructural features that suggest increased intensity of deformation towards the middle portion of the shear-zone. Further, the lower *P*′ values in the protomylonite indicate absence of deformation outside the shear-zone.

Ellipticity (*E*) values are used to understand the degree of deformation in the shear-zone and the analyses reveal that high *E* values are associated with samples falling in the shear-zone proper (Table.1). The Jelinek plot (*P*′ vs *T*) graphically displays the shape of magnetic susceptibility ellipsoids in the samples (Jelinek, 1981). In the study area, the scattered nature of *T* values with respect to *P*′ documents L-S tectonites (Fig. 9b). *P*′ values depend on the mean magnetic susceptibility (K_m) of the sample, which is

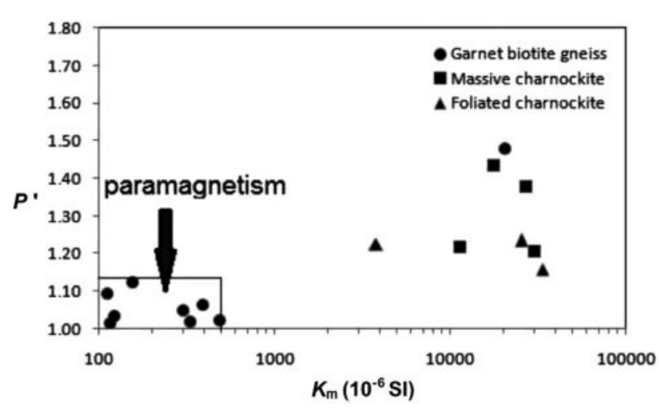

Fig. 10. K_m vs *P*′ plots for different rocks of the study area.

controlled by the volume percentage of ferrimagnetic minerals present in the rocks rather than strain alone. The K_m vs P' graph (Fig. 10) has been plotted for the undeformed, less deformed and strongly deformed rocks of the study area. The correlation of P' vs K_m is more or less weak and linear at susceptibilities lesser than 1000 μSI. All the garnet biotite gneiss samples (except sample no. V.20) plot in the field of paramagnetic minerals suggesting the predominance of paramagnetic minerals in gneissic rocks (Fig. 10). Sample no.V.20 falls outside the field of paramagnetic minerals indicating the dominance of ferrimagnetic minerals like magnetite in the sample. Similar observations are noted by Ferŕe et al. (2003, 2004) for the migmatites of the Superior province of Canadian shield. Massive charnockite and foliated charnockite samples display magnetic properties outside the field of paramagnetic minerals indicating the dominance of ferrimagnetic minerals in the samples. But the negative correlation noted in few charnockite samples is mainly due to the paramagnetic contribution such as hypersthene (Fig. 5a) and biotite. Our observations are in concordance with the relations noted by Pratheesh et al. (2012) based on their magnetic fabric studies of charnockite samples from the Moyar shear-zone of South India.

6.3. Magnetic fabric analysis

Magnetic lineations (K_1) are well organized and consistent with the field orientation measured from the AKSZ, reflecting the relation between the regional strain/kinematics and fabric development in the rocks. Contoured equal area projection of field lineation and magnetic lineation in the study area are shown in Fig. 11a and b. The orientation diagram of the magnetic lineation (K_1) recorded in the rock types of the study area shows maximum plunging in NNW direction. The mean magnetic lineation plunges 60/348 which is similar to that of the stretching lineation of the gneissic rocks and the orientation of D_1 and D_2 fold axes lineation in the gneiss. Contoured equal area projection of poles to field foliations and magnetic foliations are also shown in Fig. 11c and d. In most of the localities, the magnetic foliations present in the rocks are more or less parallel to field foliations. Mean orientation of the magnetic foliation pole (K_3) shows a distinct SW plunge (48/240) and the corresponding plane shows a general NW-SE trend consistent with that of the Achankovil shear-zone. At few locations, there is lack of correspondence between the magnetic and field data.

7. Kinematic indicators

The simplest and best known shear sense indicator is the displacement of markers such as dykes, veins, xenoliths and bedding along a shear (Simpson and Schmid, 1983; Passchier and Trouw, 2005). Quartzite and pegmatite veins in the study area are subjected to relative offset along minor shears and their sense of slip has been determined as dextral (Fig. 12a). Mesoscopic shears showing both dextral (Fig. 12b) and sinistral shear sense are well developed in the sheared gneiss and mylonites of AKSZ. The rotation of pre-existing foliation at the edge of the minor shear-zone (Simpson and Schmid, 1983) indicates the shear sense as dextral. In addition, rotated asymmetric tectonic inclusions (Fig. 12c), asymmetric clast with tails, microfaulted megacrysts of quartz grains, Z-shaped asymmetric drag folds, and tight intrafolial folds exhibit SE directed dextral shearing. However, S-C fabrics (Fig. 4c) as well as asymmetric retort shaped quartzofeldspathic augens with recrystallised tails (Fig. 12d), at places, also point to sinistral movement. Porphyroclasts with recrystallised tails are extremely important for shear sense determination in high strain zones (Simpson and Schmid, 1983; Passchier and Trouw, 2005). The stair stepping relation shown by tails of recrystallised material with respect to central porphyroclast in mantled porphyroclast systems like δ-type indicates dextral shearing (Fig. 5b). Mica fish, with the characteristic monoclinic shape symmetry are common in ductile shear zones (Simpson and Schmid, 1983). The asymmetry of dragged out mica porphyroclasts (Fig. 5b), asymmetry of the quartz sigmoids (Fig. 5c), slippage of fragments of large porphyroclast of K-feldspar along grain scale faults and quartz fabric diagrams (Fig. 7) are consistent with dextral sense.

8. Microstructural evolution and deformation mechanisms

The degree of mylonitisation varies from place to place, in the domain of a thin section to the scale of a map. The variation in the degree of deformation is indicated by the wide range in size of quartz grains in the rock. Undulatory extinction, patchy extinction and core and mantle microstructure indicate a progressive misorientation of the crystal lattice. Development of recrystallised grains around rims of quartz and the characteristic undulose extinction shown by quartz grains is indicative of dislocation glide/creep process. Sub grain formation, wavy extinction and the development of quartz ribbons suggest that dislocation creep accompanied by dynamic recrystallisation form the dominant deformation mechanism producing steady flow in the rock (White, 1976) which led to grain refinement. The curved and lobate grain boundaries between quartz and feldspar at high temperature metamorphic conditions in sheared gneisses also may be taken as an evidence for grain boundary sliding and solid state diffusion creep experienced by mineral grains (Gower and Simpson, 1992; Passchier and Trouw, 2005).

The mylonite grades to ultramylonite with increase in recrystallisation and grain size reduction associated with shearing. Fluid influx associated with shearing results in extensive biotisation of mylonites and ultramylonites. Healed up late intragranular fractures filled up with smaller recrystallised quartz grains indicate late pulse of brittle deformation. The presence of various reaction textures, coronas and symplectitic intergrowths of cordierite, K-feldspar and quartz after orthopyroxene and garnet in the rocks of the AKSZ are indicators of near isothermal decompression and rapid uplift (Santosh, 1987). The grain size reduction in minerals of the rocks of the study area would cause a change in the deformation mechanisms from dislocation creep through grain boundary sliding to grain size dependent diffusional flow, leading to strain softening.

9. Discussion

The LPO of amphibole, biotite and feldspars (Fig. 6b–e) from the AKSZ are typical of medium to high grade rocks and suggest that these minerals have been deformed plastically through the activation of intracrystalline slip systems. In *biotite* fabric diagrams, the formation of peripheral girdle with girdle axis coinciding Y is a commonly observed pattern (Turner and Weiss, 1963; Prasannakumar and Lloyd, 2007). The plane normal to the compact maximum coincides with foliation, suggesting the synchronous formation of biotite and F_1 folds. However, biotite has outlived F_1 phase of D_I deformation locally and the spread of poles to (001) can be attributed to rotation of flakes of biotite during later generation of folding and shearing events. The pole figures are characteristic of slip on both (001)[100] and (001)[010] and the strength of these LPO is due to mechanical as well as crystal plastic effects. As the flow plane and flow direction coincide with (100) and [001] respectively, the *hornblende* fabric is consistent with activation of the (100)[001] slip system similar to biotite fabric (e.g. Egydio-Silva et al., 2002). The LPO could be described as a (100)-fibre

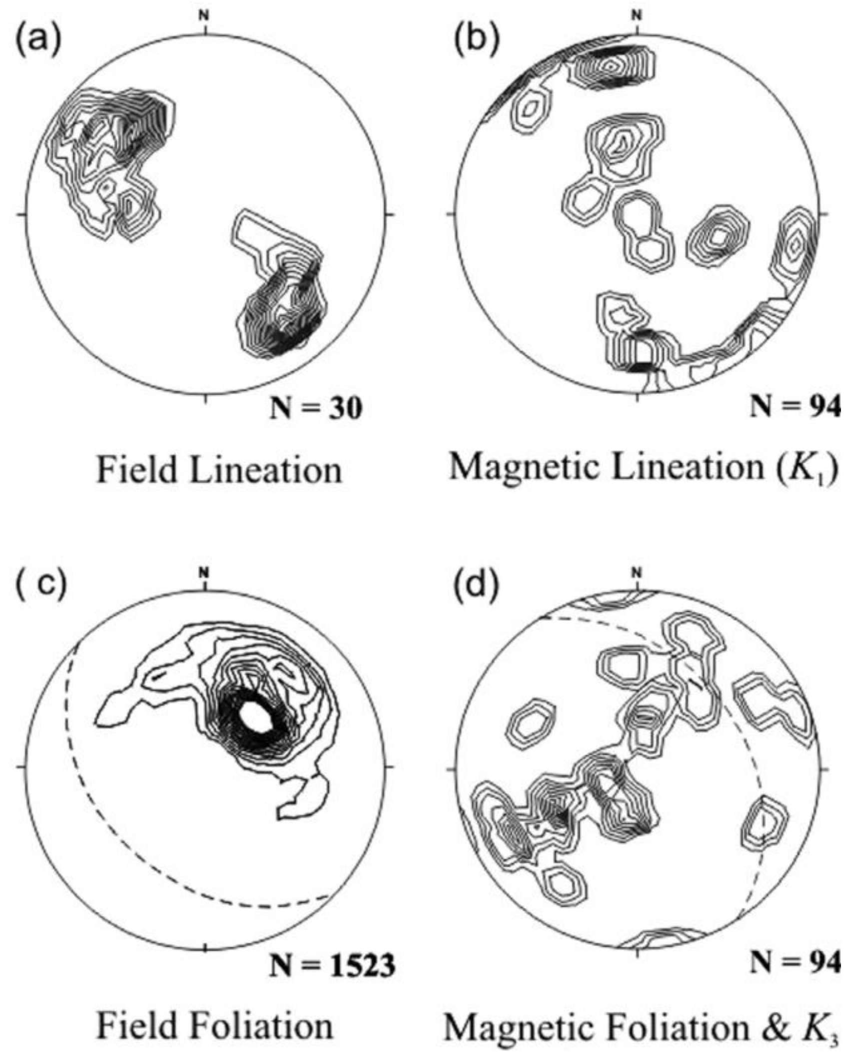

Fig. 11. Contoured lower hemisphere equal area projection of (a) field lineation (b) magnetic lineation (c) poles to field foliation and (d) magnetic foliation in the rocks of the study area. Dashed great circles in (c) and (d) represent the mean orientation of the foliation.

texture based on the analogy with the olivine fabric data (Ben Ismail and Mainprice, 1998) and hence may also indicate slip on (100)[010]. Rigid body rotation has been considered to play a vital role in the LPO development of hornblende and biotite (Diaz Aspiroz et al., 2007; Prasannakumar and Lloyd, 2010). Grains are rotated towards the XY plane of the finite strain ellipsoid during deformation (Passchier and Trouw, 2005), such that the amphibole (100) and biotite (001) planes become parallel to the macroscopic foliation. Moreover, due to the similarity between the grain and crystal shapes of these minerals, the biotite [100] and amphibole [001] directions also are rotated towards the X tectonic direction to define the macroscopic stretching lineation. In contrast, the quartz LPO is unusually weak and may represent annealing of a microstructure that developed via diffusional rather than dislocation creep processes following significant grain size reduction and subsequent annealing. Alternatively, it may represent a combination of fabrics developed in different deformation events such that quartz LPO of the mylonite is characterised by reduction of LPO intensity compared to the protolith. The general tectonic set up of the AKSZ rocks indicates polyphase deformation and metamorphism suggesting possibility of reactivation of the shear-zone. Hence it is probable that the fabric and LPO reflect the modifications by repeated events with one of the events dominating in fabric development.

Magnetic fabric data obtained from the gneissic rocks show significant correlation with the field and micro fabrics. Pole to foliation derived from field data and AMS analysis (K_3- pole to magnetic foliation) are identical. Similarly the orientation of the magnetic lineation (K_1) is also consistent with the attitude of field lineation. In few locations, there is lack of correspondence between the field and magnetic data which could be due to the effect of subsequent deformation phase. It is clear from the magnetic susceptibility (both bulk susceptibility and anisotropy degree) and the magnetic fabric data that the magnetic susceptibility of gneissic rocks from the AKSZ is controlled predominantly by the deformed paramagnetic minerals with a minor ferrimagnetic phase aligned parallel to the regional trend of shear-zone. The wide variation in the susceptibilities of charnockites can be explained on the basis of changes in magnetic mineralogy during prograde and retrograde metamorphic processes.

Microstructural analysis of the shear-zone fabrics supports a general dextral sense of tectonic transport in AKSZ. However, there are domains and microdomains characterised by sinistral shear as opposed to the dextral bulk shear and are confined to high strain zones particularly in the middle or central part of the shear-zone. The orientation of flattening plane (XY) and maximum extension direction (X) is almost consistent in different micro domains even though zones of different shear sense exist.

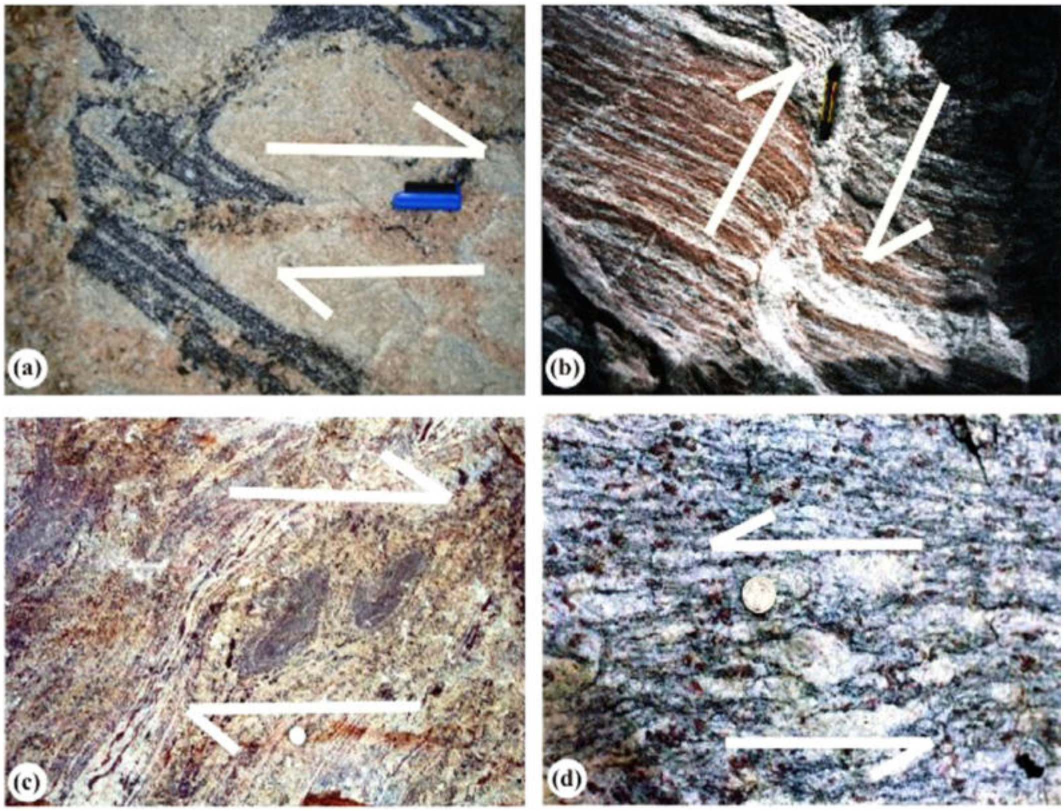

Fig. 12. Mesoscopic kinematic indicators in the study area: (a) Offset of veins along minor shear defining dextral shear sense (Inclined section). (b) Minor dextral shear developed in gneiss. Quartzite vein is seen intruded parallel to shear plane (Inclined section). (c) Folded and sheared pyroxene granulite boudins in gneiss showing dextral sense (Inclined section). (d) Asymmetric augens in sheared gneiss showing sinistral sense of shearing (Inclined section).

The intensity of deformation increases towards the central part of the AKSZ from the periphery as evidenced by the spatial grading of rocks, particularly the sheared gneisses with mylonites in the centre of the shear-zone to massive charnockite and garnet biotite gneiss on either side of the shear-zone. The progressive strain gradient in the terrain is evident in the rotation of C-bands into parallelism with the foliation planes due to progressive shearing resulting in a complex mylonitic fabric. Based on microstructural analysis, a progressive change in the deformation mechanisms from dislocation creep through grain boundary sliding to grain size dependent diffusional flow has been observed in the study area. The strain partitioning and/or reactivation of the AKSZ during Pan African times can be treated as the reason for the diverse shear sense noticed in the study area i.e., the AKSZ had undergone an initial ductile dextral deformation during D_2 and was reactivated and superimposed by sinistral movements in D_3.

10. Conclusion

The AKSZ in the SGT exhibits complex structural features with diverse kinematic indicators at different scales of observations. A strong, tectonic L-S fabric has developed all along the AKSZ characterised by grain size reduction, flattening, elongation and dimensional preferred orientation of quartz, biotite, hornblende, plagioclase and orthoclase, corresponding to a progression in strain. EBSD derived quartz LPO suggests diffusional creep accommodated deformation whereas mica, amphibole and feldspars indicate plastic deformation through the activation of intracrystalline slip systems. All LPO suggest modifications in the fabric due to the reactivation during the tectono-thermal history of the shear-zone. The anisotropy of magnetic susceptibility of sheared gneissic rocks is predominantly controlled by the deformed paramagnetic minerals with a minor ferrimagnetic phase aligned parallel to the regional trend of AKSZ. Magnetic lineation (K_1) and foliation pole (K_3) are consistent with the field orientation and LPO, reflecting the relation between the regional strain/kinematics and fabric development in the rocks. The progressive evolution of mylonite causes a change in the deformation mechanisms from dislocation creep through grain boundary sliding to grain size dependent diffusional flow in the study area. Kinematic indicators on meso- and microscopic scales point to dominant dextral sense of shearing. However, evidences in favour of a sinistral shear are also obtained from micro domains in the shear-zone. Opposing shear sense is interpreted as the product of strain partitioning and/or reactivation of the shear-zone during Pan African time. The bulk kinematic model suggests that the shearing in AKSZ took place with WNW-ESE to NW-SE trending flattening plane (XY) in a NNE-SSW to NE-SW compressive field. The tectonic models proposed for Pan-African orogenesis in South India will need to accommodate the dominant dextral strike slip shearing movement of the AKSZ.

Acknowledgements

The first author acknowledges the financial support provided by CSIR, India under CSIR-JRF scheme. This contribution forms a part of the doctoral work of CV. Authors are grateful to the anonymous referees for their thorough reviews that greatly improved the quality of the manuscript.

References

Archanjo, C.J., Launeau, P., Bouchez, J.L., 1995. Magnetic fabric vs. magnetite and biotite shape fabrics of the magnetite-bearing granite pluton of Gamelerias (Northeast Brazil). Phys. Earth Planet. Inter. 89, 63–75.

Ben Ismail, W., Mainprice, D., 1998. An olivine fabric database: an overview of upper mantle fabrics and seismic anisotropy. Tectonophysics 296, 145–158.

Brandon, A.D., Meen, J.K., 1995. Nd isotopic evidence for the position of southernmost Indian terranes within East Gondwana. Precambr. Res. 70, 269–280.

Bunge, H.J., 1982. Texture Analysis in Materials Science. Butterworths, London. 599 p.

Chetty, T.R.K., Bhaskar Rao, Y.J., Narayana, B.L., 2003. A structural cross-section along Krishnagiri-Palani Corridor, Southern Granulite Terrain of India. In: Ramakrishnan (Ed.), Tectonics of Southern Granulite Terrain, Kuppam-Palani Geotransect, vol. 50. Geological Society of India Memoir, pp. 255–277.

Diaz Aspiroz, M., Lloyd, G.E., Fernandez, C., 2007. Development of lattice preferred orientation in clinoamphiboles deformed under low-pressure metamorphic conditions. A SEM/EBSD study of metabasites from the Aracena metamorphic belt (SW Spain). J. Struct. Geol. 29, 629–645.

Drury, S.A., Holt, R.W., 1980. The tectonic frame work of South India. A reconnaissance involving LANDSAT Imagery. Tectonophysics 65, 1–15.

Drury, S.A., Harris, N.B.W., Holt, R.W., Reeves-Smith, G.J., Wightman, R.T., 1984. Precambrian tectonics and crustal evolution in South India. J. Geol. 92, 3–20.

Egydio-Silva, M., Vauchez, A., Bascou, J., Hippertt, J., 2002. High-temperature deformation in the Neoproterozoic transpressional Ribeira belt, southeast Brazil. Tectonophysics 352, 203–224.

Ferŕe, E.C., Teyssier, C., Jackson, J., Thill, J.V., Rainey, E.S.G., 2003. Magnetic susceptibility anisotropy: a new petrofabric tool in migmatites. J. Geophys. Res. 108. http://dx.doi.org/10.1029/2002JB001790.

Ferŕe, E.C., Martın-Herńandez, F., Teyssier, C., Jackson, M., 2004. Paramagnetic and ferromagnetic anisotropy of magnetic susceptibility in migmatites: measurements in high and low fields and kinematic implications. Geophys. J. Int. 157, 1119–1129.

Gower, R.J.W., Simpson, C., 1992. Phase boundary mobility in naturally deformed, high-grade quartzofeldspathic rocks: evidence for diffusional creep. J. Struct. Geol. 14, 301–313.

Hrouda, F., 1993. Theoretical models of magnetic anisotropy to strain relationship revisited. Phys. Earth Planet. Inter. 77, 237–249.

Jelinek, V., 1981. Characterization of magnetic fabrics of rocks. Tectonophysics 79, 63–67.

Kumar, Niraj, Singh, A.P., Singh, B., 2009. Structural fabric of the Southern Indian shield as defined by gravity trends. J. Asian Earth Sci. 34, 577–585.

Lloyd, G.E., 1987. Atomic number and crystallographic contrast images with the SEM: a review of backscattered electron techniques. Mineral. Mag. 51, 3–19.

Michibayashi, K., Mainprice, D., 2004. The role of pre-existing mechanical anisotropy on shear-zone development within oceanic mantle lithosphere: an example from the Oman ophiolite. J. Petrol. 45, 405–414.

Passchier, C.W., Trouw, R.A.J., 2005. Microtectonics. Springer-Verlag, Berlin-Heidelberg. 371 p.

Prasannakumar, V., 1998. Kinematics of Achankovil shear-zone. Gondwana Res. 1, 407.

Prasannakumar, V., Lloyd, G.E., 2007. Development of crystallographic lattice preferred orientation and seismic properties in Bhavani shear-zone, southern India. J. Geol. Soc. India 70, 282–296.

Prasannakumar, V., Lloyd, G.E., 2010. Application of SEM-EBSD to regional scale shear-zone analysis: a case study of the Bhavani Shear-Zone, South India. J. Geol. Soc. India 75 (1), 183–201.

Pratheesh, P., Prasannakumar, V., Praveen, K.R., 2012. Magnetic fabrics in characterization of magma emplacement and tectonic evolution of the Moyar Shear Zone, South India. Geosci. Front. 4, 113–122.

Prior, D.J., Boyle, A.P., Brenker, F., Cheadle, M.C., Day, A., Lopez, G., Potts, G.J., Reddy, S., Spiess, R., Timms, N., Trimby, P., Wheeler, J., Zetterstrom, L., 1999. The application of electron backscatter diffraction and orientation contrast imaging in the SEM to textural problems in rocks. Am. Mineral. 84, 1741–1759.

Radhakrishna, T., Mathai, J., Yoshida, M., 1990. Geology and structure of the high-grade rocks from Punalur-Achankovil sector, south India. J. Geol. Soc. India 35, 263–272.

Raharimahefaa, T., Kusky, T.M., 2010. Temporal evolution of the Angavo and related shear- zones in Gondwana: Constraints from LA-MC-ICP-MS U-Pb zircon ages of granitoids and gneiss from central Madagascar. Precambr. Res. 182 (1–2), 30–42.

Rajaram, M., Anand, S.P., 2014. Aeromagnetic signatures of Precambrian shield and suture zones of Peninsular India. Geosci. Front. 5, 3–15.

Rajaram, M., Harikumar, P., Brown, M., 2003. Thin magnetic crust in the Southern Granulite Terrain. In: Ramakrishnan, M. (Ed.), Tectonics of Southern Granulite Terrane, vol. 50. Geological Society of India Memoir, pp. 165–176.

Rajesh, K.G., Chetty, T.R.K., 2006. Structure and tectonics of the Achankovil Shear-Zone, Southern India. Gondwana Res. 10, 86–98.

Rajesh, H.M., Santosh, M., Sekhar, S.B., Shaju, K.M., 1998. The Achankovil Shear-Zone, Southern India: evidence for Sinistral Shearing. Indian Miner. 32 (1), 17–23.

Rathore, J.S., 1980. The magnetic fabrics of some slates from the Borrowdale volcanic group in the English lake district and their correlations with strain. Tectonophysics 67 (3–4), 207–220.

Reddi, A.G.B., Mathew, M.P., Singh, B., Naidu, P.S., 1988. Aeromagnetic evidence of crustal structure in the granulite terrain of Tamilnadu-Kerala. J. Geol. Soc. India 32, 368–381.

Sacks, P.E., Nambiar, C.G., Walters, L.J., 1997. Dextral Pan-African shear along the South western Edge of the Achankovil Shear Belt, South India: constraints on Gondwana Reconstructions. J. Geol. 105, 275–284.

Santosh, M., 1987. Cordierite gneisses of Southern Kerala, India: petrology, fluid inclusions and implications for crustal uplift history. Contrib. Miner. Petrol. 96, 343–356.

Schmidt, N.H., Olesen, N.Ø., 1989. Computer-aided determination of crystal-lattice orientation from electron channelling patterns in the SEM. Can. Miner. 27, 15–22.

Simpson, C., Schmid, S.M., 1983. Microstructural indicators of sense of shear in shear zones. Bull. Geol. Soc. Am. 94, 1281–1288.

Sinha Roy, S., Mathai, J., Narayanaswamy, S., 1984. Structure and metamorphic characteristics of cordierite bearing gneisses of south Kerala. J. Geol. Soc. India 25, 231–234.

Srikantappa, C., Raith, M., Spiering, B., 1985. Progressive charnockitisation of the leptynite – khondalite suite in Southern Kerala, India – evidence for formation of charnockites through a decrease in fluid pressure? J. Geol. Soc. India 26, 859–872.

Tarling, D.H., Hrouda, F., 1993. The Magnetic Anisotropy of Rocks. Chapman & Hall, London. 217 p.

Turner, F.J., Weiss, L.E., 1963. Structural Analysis of Metamorphic Tectonites. Mc Graw Hill, New York. 545 p.

White, S.H., 1976. The role of dislocation processes during tectonic deformation with special reference to quartz. In: Strens, R.J. (Ed.), The Physics and Chemistry of Minerals and Rocks. Wiley, London, pp. 75–91.

Windley, B.F., Razafiniparany, A., Razakamanana, T., Ackermand, D., 1994. Tectonic framework of the Precambrian of Madagascar and its Gondwana connections: a review and reappraisal. Geol. Rundsch. 83, 642–659.